BAMS Filtering and Applications to Denoising Ozone Concentration Measurements

Gabriel Katul
Duke University
Durham, NC 27708-0251, USA

Fabrizio Ruggeri
CNR - IAMI
I-20131 Milano, Italy

Brani Vidakovic
Georgia Institute of Technology
Atlanta, GA 30332-0205, USA

Abstract

We propose a method for filtering self-similar geophysical signals corrupted by an autoregressive noise using non-decimated wavelet transforms and Bayesian model in the wavelet domain. In the application part, we consider separating the instrumentation noise from high frequency ozone concentration measurements sampled in the atmospheric boundary layer. The elicitation of priors needed to specify the statistical model in this application is guided by the well-known Kolmogorov **K41**-theory, which describes the spectral power laws of the high frequency scalar concentration fluctuations.

Gabriel Katul is an Associate Professor at the School of the Environment, Duke University, Durham, NC 27708-0251, USA.

Fabrizio Ruggeri is a Senior Researcher at Consiglio Nazionale delle Ricerche, Istituto per le Applicazioni della Matematica e dell'Informatica, Via A. M. Ampere, 56, I-20131 Milano, Italy.

Brani Vidakovic is an Associate Professor at the School of Industrial and Systems Engineering, Georgia Institute of Technology, Atlanta, GA 30332-0205, USA.

This research was supported in part by NSF Grant DMS-0072585 at Duke University and Georgia Institute of Technology.

KEY WORDS: Wavelet Regression; Shrinkage; Adaptivity; Bayesian Models.

1 Introduction

Statistical modeling in the wavelet domain results in an effective shrinkage method because a prior information about the time series can be naturally incorporated in the space of associated wavelet coefficients. Prime examples are smoothness, periodicity, and self-similarity properties. According to the Bayesian approach a coherent incorporation of information can be done by appropriate selection of model components. For instance, to incorporate information about signal smoothness, variances in the prior on the signal part should decay to zero rapidly. If information about self-similarity is available, then the variances in the prior should decay in a power-law fashion.

A variety of geophysical measurements possess inherited self-similarity over a wide range of time scales; for example, turbulent velocities, temperatures and trace gas concentration in the atmospheric boundary layer follow the celebrated Kolmogorov's **K41** scaling (Kolmogorov, 1941) for locally homogeneous and isotropic turbulence. Simply stated, the spectrum of such time series exhibits a power-law decay of $-5/3$. This power-law is clearly visible in the wavelet domain when logarithms of averaged level energies are plotted against the level numbers. A large body of research connecting wavelets, geophysical time series, and their Fourier spectra exists; see for example Farge (1992), Farge *et al.* (1992), Hudgins, Friehe, and Mayer (1993), Katul and Vidakovic (1998), Kumar and Foufola-Georgiou (1993, 1994), Vattay and Harnos (1994), Vergassola, and Frisch (1991), and Zubair, Sreenivasan, and Wickerhauser (1990).

This abundance of scaling prior information in geophysical measurements is amenable to Bayesian modelling (e.g., Berliner, Wikle and Milliff, 1999; Wikle, Berliner and Cressie, 1998; Vidakovic, Katul, and Albertson, 2000). Links between Bayesian modelling and wavelet shrinkage summarizes aforementioned prior information into a sensible and effective paradigm for signal filtering and estimation. The critical fact is that, under mild conditions, Bayes rules are shrinkers and their application on wavelet coefficients leads to simple and effective estimators of unknown signals; see an example in Vidakovic and Ruggeri (1999).

In the application part, we explore the use of a Bayesian model, calibrated by exact theoretical power laws, to analyze high frequency ozone concentrations measurements contaminated with instrumentation noise at multiple frequencies. The Bayesian model is applied in the wavelet domain with the goal of separating the desired turbulence signal from inherited instrumentation noise. The proposed Bayesian model relies on BAMS (Bayesian Adaptive Multiresolution Shrinker), a technique recently proposed by Vidakovic and Ruggeri (2001). The smooth shrinkage, as opposed to thresholding, is critical in preserving the fractality if the signal. Gas analyzers used in high frequency sampling of ozone concentration tend to convolve the signal with a noise assumed either white or autoregressive. The separation between signal and noise is achieved by inverting wavelet coefficients, split in a fashion dictated by the statistical model which

incorporates a **K41** type-power law.

The paper is organized as follows: in Section 2.1 we present the underlying geophysical theory, the experiment conducted at Duke University and describe the gathered data, along with discussion on why the proposed filtering is practical. Sections 2.2 and 2.3 introduce the statistical model, the BAMS technique, and the specification of model parameters, while a more detailed description of BAMS rules is given in the Appendix. Batteries of tests, as reported in Section 3, are applied on the split components, both the signal and the noise part. The signal part is tested against the **K41** theory while the structure of the noise is analyzed for conformity with the physical properties of the instrument. Some concluding remarks, in direction of future research, and comparisons with existing methods are finally illustrated in Section 4.

2 BAMS

We review BAMS, a technique proposed in Vidakovic and Ruggeri (2001) to statistically estimate wavelets coefficients, corresponding to the signal of interest, using a shrinkage rule in a Bayesian framework. The details are postponed to the Appendix A. We start with the description of measurements.

2.1 Ozone Data

High frequency ozone concentration measurements along with the three velocity components (U, V, W) were collected at 40 m from the ground surface over a 33 m tall, 180 year old mixed hardwood forest. These experiments, performed at the Blackwood Division of Duke Forest in Durham, North Carolina, resulted in 60 1/2-hour runs (Katul *et al.*, 1997b; Katul and Albertson, 1998). We used such runs, collected over different atmospheric stability conditions, to evaluate the proposed algorithm. The fast-response O_3 gas analyzer employs chemiluminescent reaction of O_3 with eosine-Y dye borne in a carrier of ethylene glycol to measure O_3 concentration at high frequencies (Ray *et al.*, 1986; Katul *et al.*, 1996). However, the chemiluminescent reaction of O_3 with eosine-Y decreases appreciably the signal-to-noise ratio (SNR) of such gas analyzers thus prohibiting effective use of these measurements to investigating higher-order turbulence moments (Lenschow, 1982) or organized eddy motion responsible for the exchange of O_3 between the forest and the atmosphere.

2.2 The Bayes rule

Suppose the observed data $\mathbf{y}$ represent the sum of an unknown signal $\mathbf{s}$ and random noise ϵ. Coordinate-wise,

$$\mathbf{y}_i = \mathbf{s}_i + \epsilon_i', \ i = 1, \ldots, n. \tag{1}$$

In the wavelet domain (after applying a nondecimated wavelet transformation W to the observed data), expression (1) becomes $d_{jk} = \theta_{jk} + \epsilon_{jk}$, where d_{jk}, θ_{jk}, and ϵ_{jk} are the j,k-th coordinates in the traditional nondecimated scale/shift wavelet-enumeration of vectors $W\mathbf{y}, W\mathbf{s}$ and $W\epsilon'$, respectively. Our assumption is that the coefficients d_{jk} can be considered independently, at least for high resolution levels, since the wavelet transformations are generally decorrelating. When modeling in practice, such assumption prove to be reasonable. In the exposition that follows, we omit the double index jk and work with a "typical" wavelet coefficient, d. A brief overview of nondecimated wavelet transformations is given in the Appendix B.

It is now standard practice in model-induced wavelet shrinkage to specify a location model on the wavelet coefficients, elicit the prior on their locations (the signal part in wavelet coefficients), exhibit the Bayes estimator for the locations and, if the resulting Bayes rules are shrinkage estimators, apply the inverse wavelet transformation to the estimators.

We assume, as commonly done, that each coefficient d in the wavelet domain is affected by normal errors, and thus the conditional distribution of d given θ and σ^2, $[d|\theta, \sigma^2]$, is $\mathcal{N}(\theta, \sigma^2)$.

In BAMS the prior distributions on σ^2 and θ are chosen to be, respectively, an exponential one, $\mathcal{E}(\mu)$, and a mixture of a point mass at zero and a double exponential distribution, $\mathcal{DE}(0, \tau)$.

The Bayes rule is:

$$\delta^*(d) = \frac{(1-\epsilon)\ m(d)\ \delta(d)}{(1-\epsilon)\ m(d) + \epsilon\ \mathcal{DE}\left(0, \frac{1}{\sqrt{2\mu}}\right)}. \tag{2}$$

where

$$m(d) = \frac{\tau e^{-|d|/\tau} - \frac{1}{\sqrt{2\mu}} e^{-\sqrt{2\mu}|d|}}{2\tau^2 - 1/\mu}.$$

Figure 5 depicts the rule in (2). Notice that this rule is close to a thresholding rule: it heavily shrinks small-in-magnitude arguments while the large ones are slightly shrunk.

BAMS method is implemented in the MATLAB toolbox of Antoniadis, Bigot, and Sapatinas (Antoniadis *et al.*, 2001) available at

`http://www-lmc.imag.fr/SMS/software/wavden/`.

2.3 Tuning the Model Parameters

One of the main issues in any Bayesian analysis is the elicitation of the hyperparameters specifying the statistical model. Often the hyperparameters may have their own priors, leading to hierarchical models.

The described model depends on 3 hyperparameters that have to be specified. Purely subjective elicitation of priors is difficult since, in general, users

may lack intuition and interpretation of wavelet-domain priors. Subjective priors can be easily elicited only when the prior information concerns smoothness or self-similarity. A variety of default solutions are available, but default choices do not seem to be very suitable in function estimation, since observations can vary tremendously and some degree of informativeness and/or data dependence should be exploited.

Vidakovic and Ruggeri (2001) proposed an empirical moment matching specification of parameters which worked well if the signal is smooth. In this paper, the parameter specification will reflect the fact that signals are self-similar with theoretically established Hurst exponent $H = 1/3$.

1. μ is the reciprocal of the mean for the prior on σ^2, or, equivalently, the square root of the precision for σ^2. We first estimate σ by a robust Tukey's $\texttt{pseudos} = (Q_3 - Q_1)/C$, where Q_1 and Q_3 are the first and the third quartile of the finest level of details in the decomposition and $1.3 \leq C \leq 1.5$. We propose $\frac{1}{\texttt{pseudos}}$ as a default value for μ; according to the Law of Large Numbers, this ratio should be close to the "true" μ.

2. ϵ is the weight of the point mass at zero in the prior on θ and should depend on level j. If the signal is smooth ϵ should be close to 1 at the finest level of detail and close to 0 at coarsest levels. In our case the signal is not smooth and no decay of ϵ is reasonable. We fixed $\epsilon = 0.5$ in all levels.

3. The parameter τ is the scale of the "spread part" in the prior (4). In the case of a double exponential prior, the variance of the signal part is $2\tau^2$. Because of assumed independence between the error and the signal parts, we have $\sigma_d^2 = 2(1-\epsilon)^2\tau^2 + 1/\mu$, where σ_d^2 is the variance of an observation d. According to **K41** exact power laws, the average energies of the signal in the wavelet domain decay in a log-linear fashion when increasing the resolution of the levels. This provides a calibration method for eliciting prior variances on the signal coefficients: they decay proportionally to $2^{(-5/3)}$.

Unlike the thresholding rules that set small wavelet coefficients to 0, the rule (2) splits the coefficients as $d = \delta^*(d) + (d - \delta^*(d)) = \hat{\theta} + \hat{\epsilon}$. The $\hat{\theta}$-part corresponds to turbulence signal and exhibits linear spectra with the slope -5/3 ($H = 1/3$) due to just described scaling. On the other hand, the noise part coefficients, $\hat{\epsilon}$, exhibit "flat" spectra, as expected.

The process of filtering is illustrated in Figures 1-3. Figure 1(a) depicts the original O_3-concentration measurements. Not only the noise is present but measurements are quantized (rounded to a small discrete set of values) by the instrument. Figure 1(b) shows the wavelet power spectra of the measurements form the (a) panel. Note flattening of the spectra for fine scales in which the energy of noise exceeds the energy of the signal.

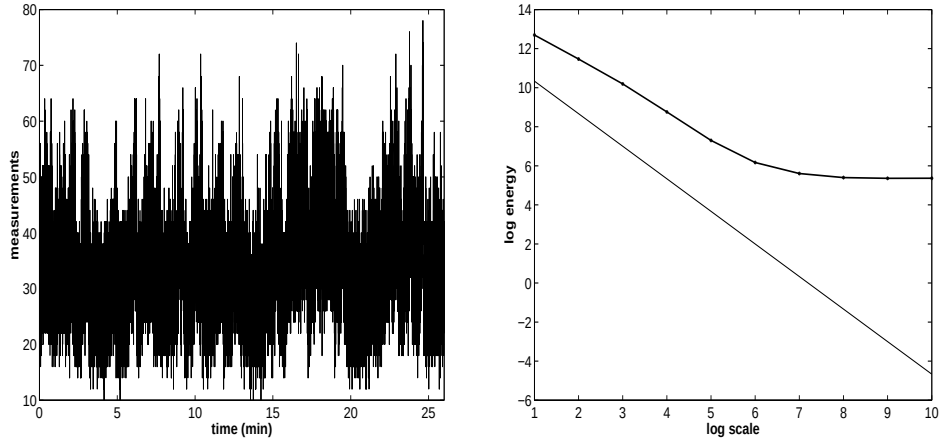

(a) (b)

Figure 1: Left: The original ozone concentration data measured at frequency of 21 Hz. Right: Wavelet-spectra suggesting that the observations contain noise (flattening of spectral line at the high resolution levels).

3 Battery of tests

The Bayes rule $\hat{\theta}(d)$ divides the wavelet coefficient in two components, $d = \hat{\theta} + (d - \hat{\theta})$. The inverse wavelet image of all $\hat{\theta}$ correspond to filtered time series, while the inverse image of $\hat{\epsilon} = d - \hat{\theta}$ corresponds to the noise component, vector $\underset{\sim}{e} = (e_1, \ldots, e_n)$ in the time domain.

The filtering algorithm must be capable of removing the noise level-wise without distorting any interaction between ozone and velocity fluctuations at multiple scales. Specifically, we tested whether (i) the wavelet cospectra between vertical velocity (W) and filtered ozone concentration follows a $-7/3$ **K41** power law, and (ii) whether the mixed structure function defined by

$$D_{UO_3O_3}(\tau) = \langle {\Delta_{O_3}}^2(\tau)\Delta_U(\tau)\rangle,$$

where angular brackets represent averaging, $\Delta_G(\tau) = G(t+\tau) - G(t)$ and G is any turbulent flow variable, follows a τ^1 power-law as in Katul *et al.* (1997a). We emphasize that the proposed battery of tests are entirely independent of the filtering scheme since they consider interactions between filtered O_3 and velocity measurements not used in the filtering scheme. Based on **K41**, the battery of tests above are applicable to any scalar fluctuations in the inertial subrange. In this experiment, air temperature fluctuations T, were also measured with high precision and hence are used as an additional line of testing on the applicability of the battery of tests (as well as **K41**) above.

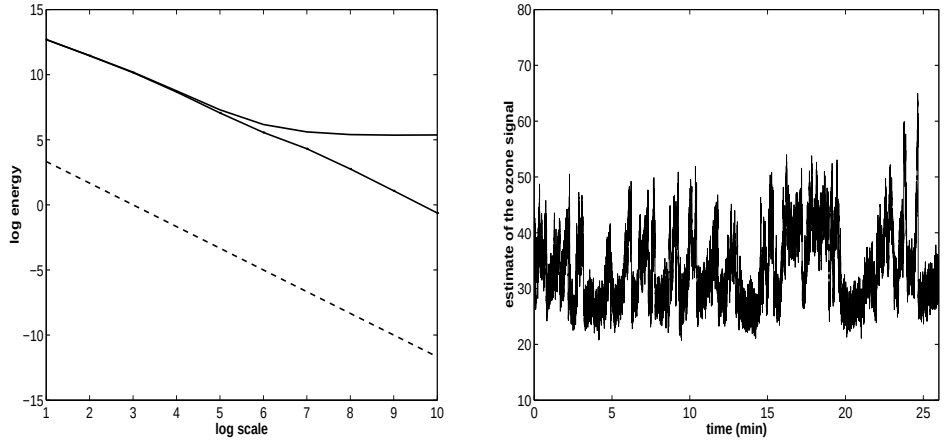

(a) (b)

Figure 2: Left: Original power spectra (from Figure 1 Right, and spectra of the estimator (almost straight line). The dotted line is the theoretical **K41** power law; Right: The estimated signal corresponding to the straight power spectra line from Left panel.

In Figure 4, the cospectra between W and the ozone time series (filtered and raw) along with **K41** power-laws and the measured cospectra between W and T, and W and U are shown for reference. It is clear that the filtering scheme did not distort the cospectral properties of W, O_3 as evidenced from their spectral similarity to W, T. However, Figure 4 clearly demonstrates that the mixed structure function $D_{UO_3O_3}(\tau)$ power-laws for the filtered O_3 time series is much closer to the measured $D_{UTT}(\tau)$ than the unfiltered O_3. Hence, the filtering scheme clearly recovered the mixed velocity-scalar moments in the inertial subrange associated with high Reynolds number flows. We note that $D_{UO_3O_3}$ is a more sensitive test because the $\Delta^2_{O_3}$ contribution to $D_{UO_3O_3}$ is more influenced by instrument noise than the influence of noise on the cospectrum between W and O_3.

In short, interactions between the filtered O_3 time series and turbulent velocity (U, W) are more consistent with theoretical predictions from turbulence theories (e.g. **K41**) than the unfiltered time series.

Although marginally normal, the residuals e_k are not exactly "white." We found that in separated noise there are significant 2- to 3-lag autocorrelations. In the run we explored the empirical model for the noise is found to be

$$e_k - 0.2971 * e_{k-1} - 0.2056 * e_{k-2} - 0.1605 * e_{k-3} = Z_n,$$

where Z_n is a white noise time series.

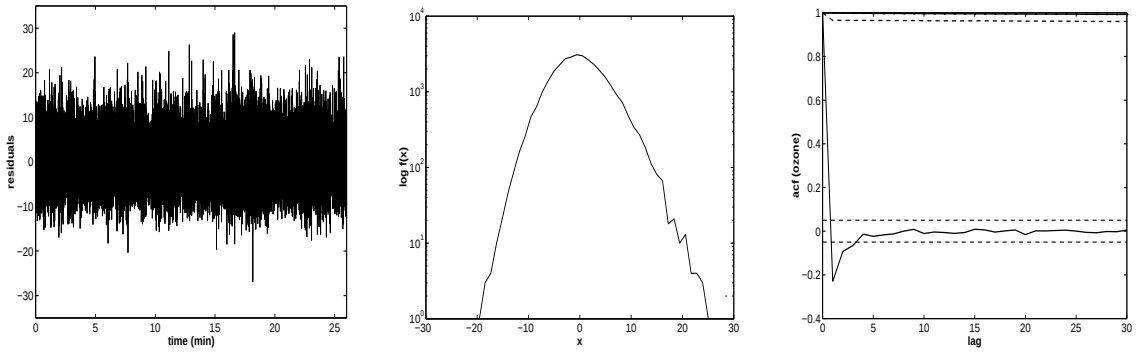

(a) (b) (c)

Figure 3: Left: Residuals (data - estimator); Center: Un-normalized density estimator for the residuals suggesting marginal normality (parabola in the log-scale); Right: Autocorrelation function (central solid line) demonstrates reasonable whiteness of the residuals. Top solid and dotted lines are autocorrelation functions of the estimator and the data, respectively.

This finding is in agreement with the physical properties of gas analyzers, in which residual reactants from previous sampling times influence the present ozone concentration measurement.

4 Conclusions

The novelty of this paper is twofold. First we have chosen nondecimated wavelet transformations in order to address the self-similarity issue locally. Although the power spectra, utilized in the BAMS method, is calculated globally, the number of local slopes used to calculate average level energies does not decrease when the levels shift from fine to coarse. This ensures more stable estimators of power spectra, especially for the coarse detail levels. In addition, there is a potential to explore self-similarity and denoise fractal signals locally by mimicking the process described in this paper for small "blocks" of coefficients.

The second novelty of the method is in its application. The BAMS method, which was tested in the case of smooth signals, is now applied to signals exhibiting fractality. Such application was enabled by a link between the geophysical phenomenon (power laws) and the prior elicitation in the model driving the BAMS method (variance decay).

Vidakovic, Katul, and Albertson (2000) considered a problem of denoising the fractional Brownian motion $fBm(1/3)$ as a model for a turbulent signal. They explored three techniques Fourier Amplitude Shrinkage (FAS) that splits Fourier coefficients ontained by FFT, Wavelet Amplitude Shrinkage (WAS) that

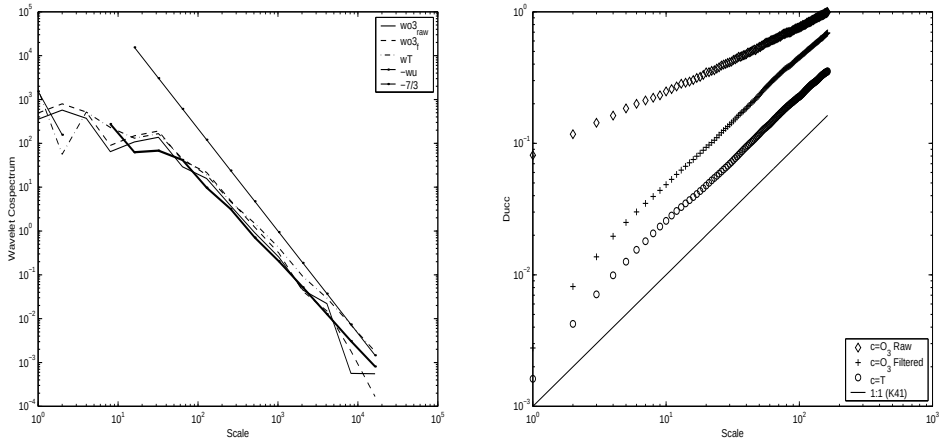

(a) (b)

Figure 4: Left: Computed Haar wavelet cospectra for filtered and raw O_3 time series with W. For reference the cospectra between W and air temperature T and W and U are shown along with **K41** power-laws. Right: Computed mixed structure functions (D_{UCC}) for C representing filtered and raw O_3 time series with U. For reference, the mixed structure function between T and U is also shown along with τ^1 from **K41**.

applies linear shrinkage on magnitudes of wavelet coefficients, and Bayesian Energy Fraction Estimation (BEFE) that uses normal model-normal prior structure in performing the filtering. Although all three methods are effective and comparable, BAMS method has 2 differences: (i) The models (marginal likelihood and prior) in BAMS are more realistic, that is, better fit the real observed data, and (ii) BAMS uses nondecimated wavelets (although critically sampled orthogonal wavelets can be used as well).

The broad outcome of this application is a filtering methodology ideally suited for disinfecting high frequency O_3 time series measurements. Such measurements can be used to infer higher-order turbulence statistics for O_3 and organized motion responsible for O_3 exchange between the forest and the atmosphere. Schemes such as surface renewal (Katul et al., 1996) can predict the O_3 fluxes from such filtered time series.

An additional potential of this approach is in dealing with multifractal (the hurst exponent H is a function if t) signals imbedded into a white noise. Preliminary research indicates good signal-noise separability as long as the "local" signal-to-noise ratio does not change much in time. This research is ongoing.

Appendices

Appendix A: Bayes Rule

The model $[d|\theta,\sigma^2] \sim \mathcal{N}(\theta,\sigma^2)$ is completed by eliciting priors on θ and σ^2. The choice of an exponential prior for σ^2 is justified since it is an entropy maximizer in the class of all distributions supported on $(0,\infty)$ with a fixed first moment. The choice of a double exponential component in the mixture point-mass prior on θ is based on inspecting the empirical realizations of coefficients of pure signals, and decision theoretical recommendations by Ruggeri and Vidakovic, (1999), whereas the point-mass-at-zero component ensures the enhanced and possibly adaptive shrinkage by the resulting Bayes rule, as shown in Vidakovic and Ruggeri (1999).

Besides, adequate changes in ϵ, the weight of the point mass, and the parameter of the double exponential distribution make it possible to adapt the shrinkage rules level-wise.

Starting with $[d|\theta,\sigma^2] \sim \mathcal{N}(\theta,\sigma^2)$ and the prior $\sigma^2 \sim \mathcal{E}(\mu), \quad \mu > 0$, with density $f(\sigma^2|\mu) = \mu e^{-\mu\sigma^2}$, we obtain the marginal likelihood

$$d|\theta \sim \mathcal{DE}\left(\theta, \frac{1}{\sqrt{2\mu}}\right), \quad \text{with density } f(d|\theta) = \frac{1}{2}\sqrt{2\mu}e^{-\sqrt{2\mu}|d-\theta|}.$$

If the prior on θ is

$$[\theta] \sim \mathcal{DE}(0,\tau),$$

then the predictive distribution of d is

$$[d] \sim m(d) = \frac{\tau e^{-|d|/\tau} - \frac{1}{\sqrt{2\mu}} e^{-\sqrt{2\mu}|d|}}{2\tau^2 - 1/\mu},$$

and the corresponding Bayes rule with respect to the squared error loss is

$$\delta(d) = \frac{\tau(\tau^2 - 1/(2\mu))de^{-|d|/\tau} + \tau^2(e^{-|d|\sqrt{2\mu}} - e^{-|d|/\tau})/\mu}{(\tau^2 - 1/(2\mu))(\tau e^{-|d|/\tau} - (1/\sqrt{2\mu})e^{-|d|\sqrt{2\mu}})}. \tag{3}$$

The rule (3) is a shrinkage one, but it is close to a linear shrinkage rule, known to be under-performing in wavelet-based methods.

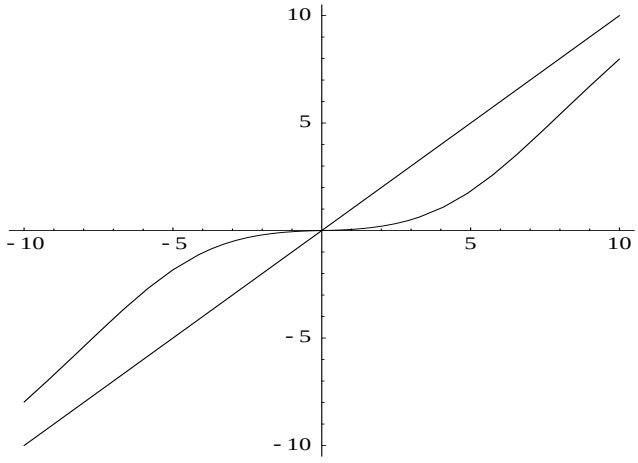

Figure 5: Bayes rule $\epsilon = 0.9, \tau = 2,\ \mu = 1/2$.

Rules with a more desirable shape result from the ϵ–contaminated priors, with a point mass at zero. When

$$[\theta|\epsilon] \sim \epsilon\delta_0 + (1-\epsilon)\mathcal{DE}(0,\tau), \tag{4}$$

the marginal is

$$d \sim m^*(d) = \epsilon\mathcal{DE}(0, \frac{1}{\sqrt{2\mu}}) + (1-\epsilon)m(d)$$

and the Bayes rule is:

$$\delta^*(d) = \frac{(1-\epsilon)\ m(d)\ \delta(d)}{(1-\epsilon)\ m(d) + \epsilon\ \mathcal{DE}\left(0, \frac{1}{\sqrt{2\mu}}\right)}.$$

This rule is depicted in Figure 5 for some specific values of hyperparameters.

Appendix B: Non-Decimated Wavelet Transformations

For quadrature mirror wavelet filters $\underset{\sim}{h}$ and $\underset{\sim}{g}$, we define recursively up-sampled filters $\underset{\sim}{h}^{[r]}$ and $\underset{\sim}{g}^{[r]}$

$$\begin{aligned} \underset{\sim}{h}^{[0]} &= \underset{\sim}{h}, \quad \underset{\sim}{g}^{[0]} = \underset{\sim}{g} \\ \underset{\sim}{h}^{[r]} &= [\uparrow 2]\ \ \underset{\sim}{h}^{[r-1]}, \quad \underset{\sim}{g}^{[r]} = [\uparrow 2]\ \ \underset{\sim}{g}^{[r-1]}. \end{aligned}$$

In practice, the dilated filter $h^{[r]}$ is obtained by inserting zeroes between the taps in $\underset{\sim}{h}^{[r-1]}$. Let $\mathbf{H}^{[r]}$ and $\mathbf{G}^{[r]}$ be convolution operators with filters $\underset{\sim}{h}^{[r]}$ and $\underset{\sim}{h}^{[r]}$, respectively. A non-decimated wavelet transformation, NDWT, is defined as a sequential application of operators (convolutions) $\mathbf{H}^{[j]}$ and $\mathbf{G}^{[j]}$ on a given time series.

Definition. *Let* $\underset{\sim}{a}^{(J)} = \underset{\sim}{c}^{(J)}$ *and*

$$\begin{aligned} \underset{\sim}{a}^{(j-1)} &= \mathbf{H}^{[J-j]}\underset{\sim}{a}^{(j)}, \\ \underset{\sim}{b}^{(j-1)} &= \mathbf{G}^{[J-j]}\underset{\sim}{a}^{(j)}. \end{aligned}$$

The non-decimated wavelet transformation of $\underset{\sim}{c}^{(J)}$ *is* $\underset{\sim}{b}^{(J-1)}$, $\underset{\sim}{b}^{(J-2)}$, $\ldots$, $\underset{\sim}{b}^{(J-j)}$, $\underset{\sim}{a}^{(J-j)}$, *for some* $j \in \{1, 2, \ldots, J\}$ *the depth of the transformation.*

If the length of an input vector $\underset{\sim}{c}^{(J)}$ is 2^J, then for any $0 \le m < J$, $\underset{\sim}{a}^{(m)}$ and $\underset{\sim}{b}^{(m)}$ are of the same length. Let $\phi_j(x) = \phi_{j,0}(x)$ and $\psi_j(x) = \psi_{j,0}(s)$. If the measurement sequence $\underset{\sim}{c}^{(J)}$ is associated with the function $f(x) = \sum_k c_k^{(J)} \phi_J(x - 2^{-J}k)$ then the kth coordinate of $\underset{\sim}{b}^{(j)}$ is equal to

$$b_{jk} = \int \psi_j(x - 2^{-J}k) f(x) dx.$$

Thus, the coefficient b_{jk} provides information at scale 2^{J-j} and location k. One can think of a nondecimated wavelet transformation as sampled continuous wavelet transformation $\langle f(x), \frac{1}{\sqrt{a}}\psi\left(\frac{x-b}{a}\right)\rangle$ for $a = 2^{-j}$, and $b = k$.

References

[1] Antoniadis, A., Bigot, J. and Sapatinas, T. (2001). Wavelet Estimators in Nonparametric Regression: Description and Simulative Comparison. Technical report IMAG, France. `http://www-lmc.imag.fr/SMS/software/wavden/wavden.pdf.zip`.

[2] Berliner, M., Wikle, C., and Milliff, R. (1999). Multiresolution wavelet analyses in hierarchical Bayesian turbulence models, In: *Bayesian Inference in Wavelet Based Models*, Eds Müller and Vidakovic, Springer-Verlag, Lecture Notes in Statistics **141**, 341–349.

[3] Farge, M. (1992). Wavelet transforms and their applications to turbulence, *Annu. Rev. Fluid Mech.*, **24**, 395–457.

[4] Farge, M., Goirand, E., Meyer, Y., Pascal, F., and Wickerhauser, M. V. (1992). Improved predictability of two-dimensional turbulent flows using wavelet packet compression, *Fluid Dynamics Research*, **10**, 229–250.

[5] Hudgins, L., Friehe, C., and Mayer, M. (1993). Wavelet Transforms and Atmospheric Turbulence, *Physical Review Letters*, **71**, 3279–3282.

[6] Katul, G.G., Finkelstein, P.L., Clarke, J.F., and Ellstad, T.G. (1996). An investigation of the conditional sampling method used to estimate fluxes of active, reactive, and passive scalars, *Journal of Applied Meteorology,* **35,** 1835–1845.

[7] Katul, G.G., Hsieh, C.I., and Sigmon, J. (1997a) Energy-inertial scale interaction for temperature and velocity in the unstable surface layer, *Boundary Layer Meteorology,* **82** 49–80.

[8] Katul, G.G., Hsieh, C.I., Kuhn, G., Ellsworth, D. and Nie, D. (1997b). The turbulent eddy motion at the forest-atmosphere interface, *Journal of Geophysical Research,* **102,** 13409–13421.

[9] Katul, G.G. and Albertson, J.D. (1998). An Investigation of higher order closure models for a forested canopy, *Boundary Layer Meteorology,* **89,** 47–74.

[10] Katul, G. and Vidakovic, B. (1998). Identification of low-dimensional energy containing/flux transporting eddy motion in the atmospheric surface layer using wavelet thresholding methods, *Journal of the Atmospheric Sciences,* **54**, 91–103.

[11] Kolmogorov, A. N. (1941). The local structure of turbulence in incompressible viscous fluid for very large Reynolds numbers, *Dokl. Akad. Nauk. SSSR,* **30**, 301–305.

[12] Kumar, P. and Foufoula-Georgiou, E. (1993). A multicomponent decomposition of spatial rainfall fields: 2. self-similarity in fluctuations, *Water Resourc. Res.*, **29**, 2533–2544.

[13] Kumar, P. and Foufoula-Georgiou, E. (1994). Wavelet analysis in Geophysics: An Introduction, In *Wavelets in Geophysics*, Eds Foufoula-Georgiou and Kumar, Academic Press, 1–43.

[14] Lenschow, D.H. (1982) Reactive trace species in the boundary layer from a micrometeorological perspective. *J. Meteorol. Soc. Japan.,* **60,** 472–480.

[15] Ray, J., Stedman, D., and Wendel, G. (1986). Fast chemiluminescent method for measurement of ambient ozone. *Anal. Chem.*,**58,** 598–600.

[16] Ruggeri, F. and Vidakovic, B. (1999). Bayesian decision theoretic approach to the choice of thresholding parameter, *Statistica Sinica,* **9**, 183-197.

[17] Vattay, G. and Harnos, A. (1994). Scaling behavior in daily air humidity fluctuations, *Phys. Rev. Lett.*, **73**, 768.

[18] Vergassola, M. and Frisch, U. (1991). Wavelet transforms of self-similar processes, *Physica D,* **54,** 58–64.

[19] Vidakovic, B., Katul, G., and Albertson, J. (2000). Multiscale denoising of self-similar processes. *J. Geophys. Res.-Atmos.* **105**, (D22) 27049–27058.

[20] Vidakovic, B. and Ruggeri, F. (1999). Expansion estimation by Bayes rules, *J. Stat. Plann. Infer.,* **79,** 223–235.

[21] Vidakovic, B. and Ruggeri, F. (2001). BAMS method: theory and simulations, Under revision for *Sankhya*.

[22] Wikle, C., Berliner, M., and Cressie, N. (1998). Hierarchical Bayesian space-time models. *Journal of Environmental and Ecological Statistics,* **5**, 117–154.

[23] Katul, G.G., C.I. Hsieh, D. Ellsworth, R. Oren, and N. Phillips (1996). Latent and sensible heat fluxes from a uniform pine forest using surface renewal and flux variance methods. *Boundary Layer Meteorology*, **80**, 249-282.

[24] Zubair, L., Sreenivasan, K., and Wickerhauser, M. (1990). Compression of turbulent data and images using wavelet packets, Yale University, New Haven.

Gabriel Katul
School of the Environment
Levine Science Research Center
Duke University
Box 90, Durham, NC 27708-0
gaby@duke.edu

Fabrizio Ruggeri
Consiglio Nazionale delle Ricerche
Istituto per le Applicazioni
della Matematica e dell'Informatica
Via A. M. Ampere, 56
I-20131 Milano, Italy
fabrizio@iami.mi.cnr.it

Brani Vidakovic
Industrial and Systems
Engineering
Georgia Institute of Technology
Atlanta, GA 30333
brani@isye.gatech.edu